



Mini review

Efficient energy transfer from polysilane molecules and its application to electroluminescence

Norihiko Kamata*, Daiyo Terunuma, Reiji Ishii, Hiroki Satoh, Satoshi Aihara, Yoshiyuki Yaoita, Shinji Tonsyo

Department of Functional Materials Science, Faculty of Engineering, Saitama University, 255 Shimo-Ohkubo, Sakura-ku, Saitama-shi, Saitama 338-8570, Japan

Received 31 December 2002; accepted 3 March 2003

Abstract

Since the first observation of an efficient resonant energy transfer between polydihexylsilane and polydiphenylsilane, we have studied the energy transfer and radiative properties of polysilanes and their energy-matched counterparts. The synthesis of soluble polysilanes enabled us to prepare such pairs in a thin film simply by a spin-coating technique. The intermolecular energy transfer from conductive poly(*m*-hexoxyphenyl)phenylsilane was utilized for electroluminescence (EL) of perylene (blue), coumarin 6 (green), 4-(dicyanomethylene)-2-methyl-6-(*p*-dimethylaminostyryl)-4H-pyran and Zinc tetra-phenylporphyrin (red). A white EL was also observed by mixing four dye molecules. Photo-oxidation during irradiating an ultraviolet light was suppressed by synthesizing water-soluble polysilanes and embedding it inside sol-gel glass matrices. These results imply that polysilanes have a possibility to open new fields of optical applications.

© 2003 Elsevier B.V. All rights reserved.

Keywords: Polysilane; Organic electroluminescence; Energy transfer; Fluorescence spectra; Wet process; Sol-gel glass**1. Introduction**

Polysilanes are high polymers having Si backbones with a variety of organic side chains. They exhibit unique properties as one-dimensional semiconductors (i.e. quantum wires) in both transport and optical characteristics due to the delocalized σ -electrons along the Si main chain [1–7]. Mobility of holes in polymethylphenylsilane is up to $10^{-4} \text{ cm}^2 (\text{V s})^{-1}$ [4], though it is not an intrinsic limit but the value determined by an intermolecular hopping. Near-ultraviolet (UV) light emission with high internal quantum efficiency [8,9] is an evidence of its superior oscillator strength originating from one-dimensional excitons.

Extensive investigations on the synthesis, fundamental properties [1–7], photo-oxidation under UV light irradiation [10], application to electroluminescence (EL)

in an UV region [2,11–14], etc. were reported from both scientific and technological aspects. Since the efficient intermolecular energy transfer between polydihexylsilane (PDHS) and polydiphenylsilane (PDPS) was observed [15,16], we have been engaged in studying the energy transfer quantitatively as well as combining and synthesizing energy-matched pair of molecules [17–19]. The synthesis of soluble poly-bis(*p*-propoxyphenyl)silane (PBPPS) [20] and poly(*m*-hexoxyphenyl)phenylsilane (PHPPS) enabled us to realize the energy transfer inside thin films by a simple spin-coating technique.

The combination of a conductive PHPPS and radiative dye molecules, perylene (blue), coumarin 6 (green), 4-(dicyanomethylene)-2-methyl-6-(*p*-dimethylaminostyryl)-4H-pyran (DCM) and Zinc tetra-phenylporphyrin (ZnTPP) (red), was utilized for EL in the visible wavelength region, together with a white EL by mixing four dye molecules [19,21,22]. Against photo-oxidation under UV light irradiation, we synthesized water-soluble polysilanes [23] and improved their durability by embedding them inside sol-gel glass matrices [24,25].

* Corresponding author. Tel.: +81-48-858-3529; fax: +81-48-858-9131.

E-mail address: kamata@fms.saitama-u.ac.jp (N. Kamata).

The possibility of realizing Si-based optical devices, therefore, became a step clearer.

2. Optical properties of polysilanes

The all-*trans* conformation of polysilanes corresponds to a unit along $\langle 110 \rangle$ direction in the crystalline Si as shown in Fig. 1. This one-dimensional configuration provides direct energy-band structure and excitonic photoluminescence (PL) takes place [1–7] with high quantum efficiency [8,9]. Such one-dimensional nature needs a series of σ -conjugated array of Si atoms called as segment. The number of Si atoms in the segment is typically 30 at most. All segments of a polysilane molecule contribute to light absorption, while the absorbed energy migrates along the Si main chain and is released as a photon at one of relatively long segments with stable electronic states.

Selection of side chains provides a variety of optical and electronic functions in a molecule as well as determining the conformation of the main chain. Dialkyl-based polysilanes emit near-UV light, while diphenyl-based polysilanes present helix conformation and have visible excitonic emission in the violet region. High oscillator strength of polysilanes is essential to both light emission and the intermolecular energy transfer.

3. Energy transfer between different polysilanes

3.1. Energy-matched donor–acceptor pair

The rate of resonant energy transfer between energy-donor and energy-acceptor depends on the energy overlap between them as well as their spatial distance [26,27]. The emission energy of an energy-donor must

coincide with the major part of the absorption spectrum in an energy-acceptor for realizing efficient energy transfer. We noticed first the energy overlap between the PL spectrum of PDHS and PL excitation (PLE) spectrum of PDPS as shown in Fig. 2.

The synthesis of PDHS and PDPS was carried out by the conventional Wurtz-type reaction of dichlorosilane. The typical molecular weight of PDHS was 12 000, which was revealed by gel permeation chromatography analysis. We mixed PDHS and PDPS in the form of powders since no solvent dissolves PDPS. Samples with PDHS–PDPS mixing ratio (in wt.%) of 20/80, 50/50 and 80/20 were brayed in a mortar and were set into a concave holder of 6.0 mm diameter and 2.0 mm depth.

Under an optical excitation of 4.0 eV, which corresponds mostly to the excitation of PDHS, PL spectra of samples with different PDHS–PDPS ratio are shown in Fig. 3. A decrease in PDHS emission and an increase in PDPS emission became clear in the mixed sample. Time resolved PL showed that the lifetime of both PDHS and PDPS emission decreased with increasing the mixing ratio of PDPS as shown in Fig. 4. The lifetime of PDHS emission decreased from 1.17 ns (without PDPS) to 0.70 ns (80% PDPS).

The lifetime shortening of energy donor is a piece of direct evidence of resonant energy transfer to the energy acceptor. In case the acceptor absorbs photons emitted from the donor, the lifetime should be independent on the acceptor concentration. Direct overlap of wavefunctions between them (exchange interaction) is excluded since they are not in a solution but mixed in the powder form. We analyzed the data based on a simplified model [16] shown in Fig. 5 and obtained the lifetime of the resonant energy transfer τ_{HP} as 0.5 ns and the efficiency of the energy transfer as high as 60% at the mixing ratio of 50/50.

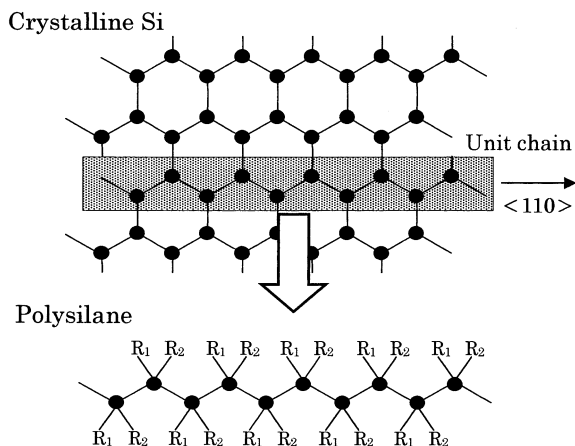


Fig. 1. The Si-backbone of a polysilane molecule which corresponds to an array of Si atoms toward $\langle 110 \rangle$ direction in the crystalline Si.

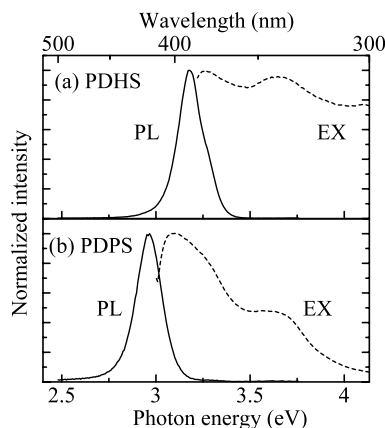


Fig. 2. PL (solid curve) and PLE (dashed curve) spectra of (a) PDHS and (b) PDPS.

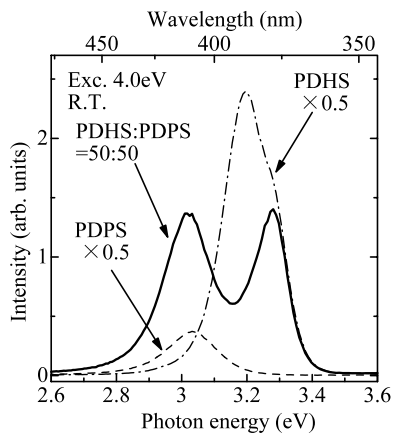


Fig. 3. PL spectrum of the equally mixed sample (PDHS–PDPS = 50/50) in comparison with that of each constituent.

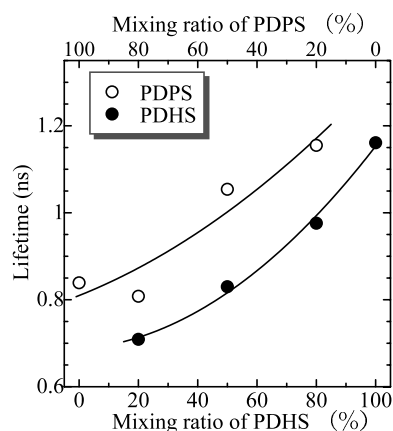


Fig. 4. Lifetimes of PDHS and PDPS emission components as a function of mixing ratio.

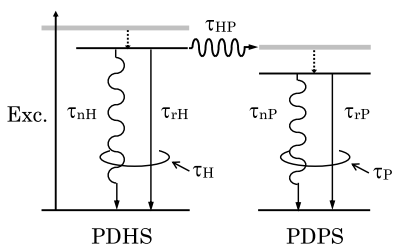


Fig. 5. Schematic illustration of the recombination and resonant energy transfer processes in the PDHS–PDPS samples.

3.2. Soluble pair in a spin-coated film

Since insolubility of PDPS in any organic solvent restricts applicability, soluble diphenyl-based polysilanes, bis(*p*-butoxyphenyl), bis(*m*-butoxyphenyl) and bis(*p*-butyl-phenyl) substituted polysilanes were synthesized [28]. We synthesized PBPPS and PHPPS as soluble candidates for energy transfer by Wurtz-type condensation with sodium metal using the method of Miller and Michl [5]. Molecular structures of them are shown in Fig. 6 together with those of PDHS and PDPS.

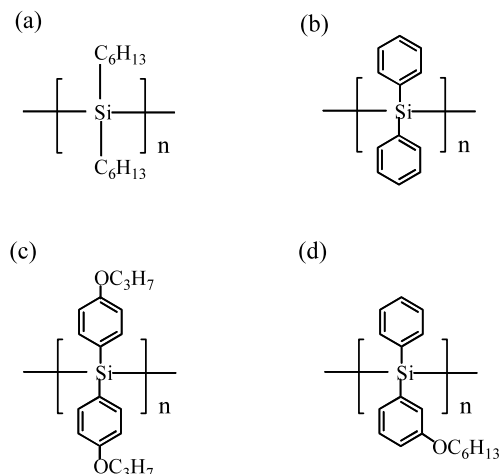


Fig. 6. Molecular structure of (a) PDHS, (b) PDPS, (c) PBPPS and (d) PHPPS.

The molecular weight of synthesized PBPPS was 145 000 (3%), 3500 (74%) and 1100 (23%) revealed by gel permeation chromatography. The energy overlap between them was confirmed as shown in Fig. 7. PBPPS in tetrahydrofuran solution (60 g l^{-1}) and PDHS in hexane solution (4 g l^{-1}) were mixed and then spin-coated on quartz substrates. The PL spectrum of the mixed film at room temperature (M1 in Fig. 8) consists of PBPPS emission (3.0 eV), *trans* (3.28 eV) and 7/3-helix (3.60 eV) components of PDHS emission.

After cooling down to 77 K in a cryostat and leaving overnight to recover to room temperature, the 7/3-helix emission disappeared (M2 in Fig. 8). In contrast, when heated up to 42°C in 30 min and then cooled down to room temperature, only the 7/3-helix emission was observed (M3 in Fig. 8). The phase transition temperature of PDHS in the solid state is around 40°C and it is thermally reversible. In our case, however, the coexistence of PBPPS molecules prevented PDHS from changing its conformation partly in response to the temperature variation. The PLE peak of the *trans*-PDHS emission (M2) is 3.35 eV as shown in Fig. 9(a),

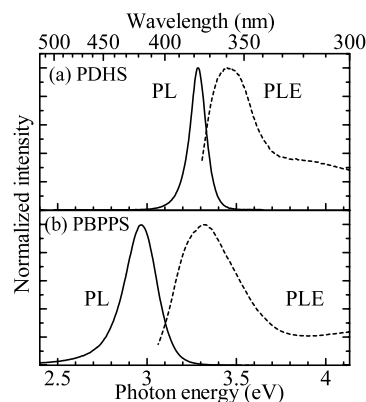


Fig. 7. PL (solid curve) and PLE (dashed curve) spectra of (a) PDHS and (b) PBPPS.

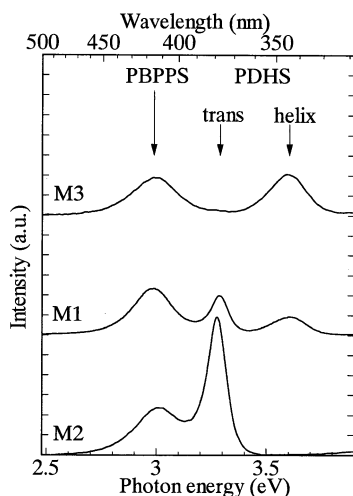


Fig. 8. The PL spectra of the PDHS–PBPPS solution-mixed film at room temperature. (M1) as prepared, (M2) after cooling cycle down to 77 K and (M3) after heating cycle up to 42 °C.

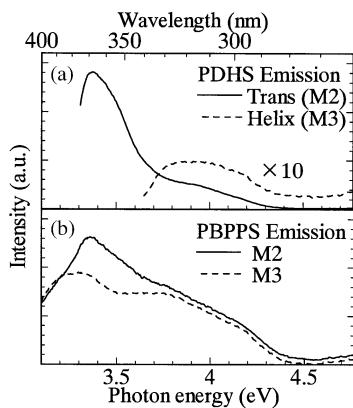


Fig. 9. The PLE spectra of (a) PDHS and (b) PBPPS emission components in solution-mixed films.

which coincided with that of the PBPPS emission (M2) shown in Fig. 9(b). The lifetime of the PDHS emission in M2 was 0.99 ns and it was shorter than that of 1.10 ns obtained by a pure film. These results imply that PDHS and PBPPS are homogeneously mixed and the energy transfer between them takes place.

4. Energy transfer to organic dye molecules

So many works were reported on organic EL applications [11–14]. As for their materials, soluble polymers have an advantage of wet process over vacuum deposition-based molecules. Taking intermolecular energy transfer into consideration, we noticed the importance of optimizing molecular pairs, especially pairs of conducting energy donors and radiative energy acceptors in the visible-wavelength region.

We used PBPPS as an energy donor and choose perylene as an energy acceptor. The energy relation

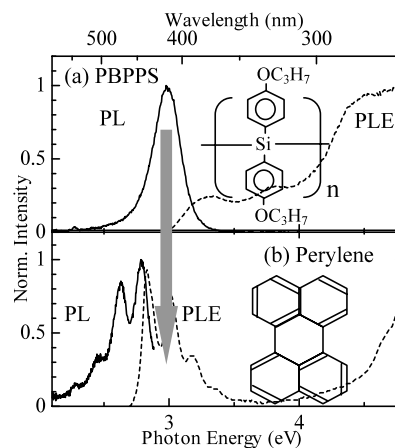


Fig. 10. PL (solid curve) and PLE (dashed curve) spectra of (a) PBPPS and (b) perylene.

between PBPPS and perylene is shown in Fig. 10. Simple spin-coating technique was used to prepare thin films of PBPPS–perylene mixture on a quartz substrate with different composition ratios. Shown in Fig. 11 is the concentration dependence of the perylene emission when PBPPS was excited. The intensity of perylene emission increased initially (that of PBPPS decreased in turn) with increasing concentration up to 0.5 mol.%, then decreased at higher concentration. In the PLE spectra of perylene emission, we can distinguish the PBPPS-originated component clearly in Fig. 12, which exemplifies the energy transfer. In this case, PMMA was used as a spacer material without interaction.

Considering PHPPS as an energy-donor, we determined energy-matched dye molecules which cover almost all visible wavelength region: They are perylene (blue), coumarin 6 (green), DCM and ZnTPP (red). The

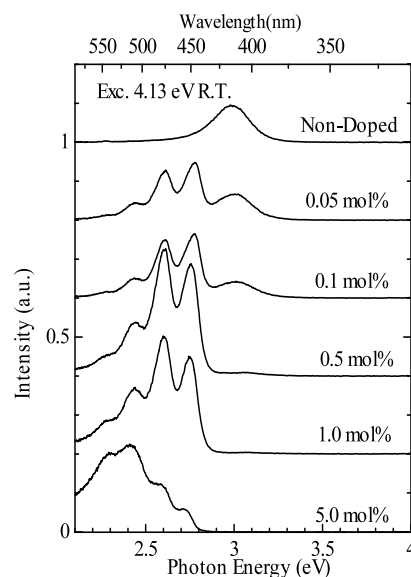


Fig. 11. PL spectra of PBPPS–perylene films as a function of perylene concentration.

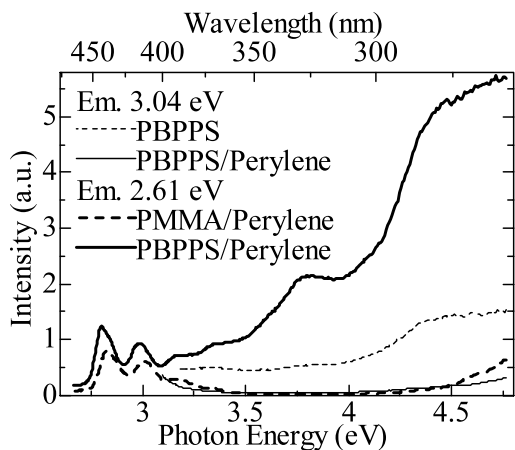


Fig. 12. PLE spectra of a PBPPS–perylene film.

molecular weight of PHPPS was 4500 (49%) and 141 000 (28%).

The combination of PHPPS and coumarin 6 is shown as an example. Spin-coated films of PHPPS with and without coumarin 6 were prepared on quartz substrates. The dye molecule was added to the chloroform solution of PHPPS (10 g l^{-1}) with the unit mole ratio of 0.5% for the film including coumarin 6. The mixed solution was then spin-coated during 1 min at 1500 rpm on a quartz substrate to form a film of 100 nm thickness. Under an optical excitation for PHPPS (4.13 eV), the PHPPS–coumarin 6 film showed a broad emission of coumarin 6 around 2.5 eV with a reduced PHPPS emission as shown in Fig. 13(a). The PLE spectrum of the coumarin 6 emission (2.56 eV) showed a distinct peak at 3.18 eV originating from that of PHPPS as shown in Fig. 13(b). Time-resolved PL measurement revealed that the lifetimes of PHPPS emission with and without coumarin 6 were 0.8 and 1.1 ns, respectively. The difference of the lifetime excludes a simple reabsorption process of photons from PHPPS. It is attributed to the resonant energy transfer.

Films of PHPPS with other dye molecules, perylene (1 mol.%), DCM (1 mol.%) and ZnTPP (0.5 mol.%), also showed similar behavior [22]. Thus we consider that the visible light emission from these dye molecules is mediated by resonant energy transfer from PHPPS.

5. Application to EL devices

5.1. Visible EL via the energy transfer

The EL device shown in Fig. 14 was fabricated firstly by spin-coating the mixed PHPPS/dye layer of roughly 100 nm onto an indium-tin-oxide coated glass substrate. Then a LiF hole-blocking layer [29] of 5 nm and Al electrode of 100 nm were deposited onto the spin-coated film in sequence, without breaking the vacuum condi-

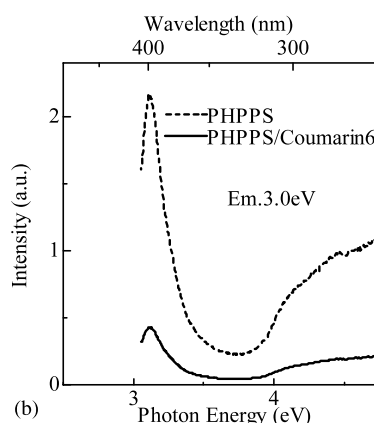
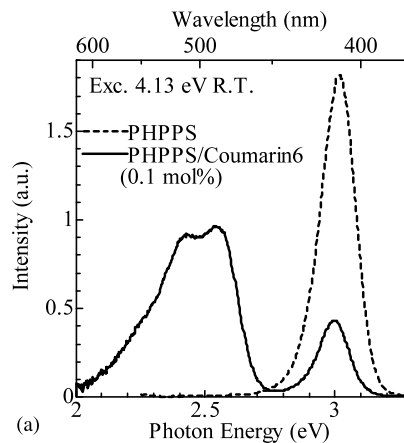


Fig. 13. (a) PL spectra of spin-coated PHPPS films with and without coumarin 6. (b) PLE spectra of PHPPS emission (3.02 eV) in PHPPS film (dashed curve) and coumarin 6 emission (2.56 eV) in PHPPS–coumarin 6 film (solid curve), respectively.

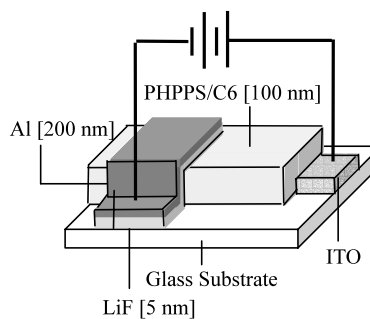


Fig. 14. The structure of a PHPPS–dye EL device.

tion. The light emitting area was 20 mm^2 . The EL spectra were measured under dc current operation at 77 K since no protective layer against oxygen and water was provided at this stage. Prior to visible EL, we confirmed that a distinct EL of PHPPS itself was observed without mixing dye molecules. The EL of PHPPS was observed up to room temperature.

We set the coumarin 6 concentration to 2 mol.% based on the concentration dependence of EL spectra

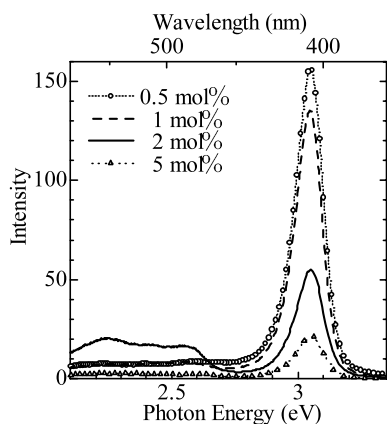


Fig. 15. EL spectra of PHPPS-coumarin 6 devices as a function of coumarin 6 concentration.

shown in Fig. 15. The current-voltage curve of the PHPPS-coumarin 6 (2 mol.%) device showed an increase of injection current and distinct EL roughly above 20 V at 77 K. Since no current was measured without PHPPS, the distinct green emission of coumarin 6 implies that the energy transfer from conducting PHPPS to coumarin 6 took place also in the EL device. In the same way, we observed visible EL at 77 K in our PHPPS-erylene (1 mol.%), PHPPS-DCM (2 mol.%) and PHPPS-ZnTPP (2 mol.%) devices as shown in Fig. 16(b-d), respectively.

5.2. White EL by intermixing dye molecules

Next to the blue, green and red EL, we tried to realize a white EL simply by intermixing these dye molecules. Perylene, coumarin 6, DCM, ZnTPP and PHPPS were intermixed into the solution by using chloroform as a solvent. The spin-coating process of PHPPS/mixed-dye layer of 100 nm thickness and following deposition of upper electrode was the same as before. An example of the EL spectrum from the dye mixture of perylene-coumarin 6-DCM-ZnTPP = 5.0:2.5:1.0:0.2 in mol.% is shown in Fig. 17. The mixed-dye EL device showed current onset above 18 V with a distinct white light

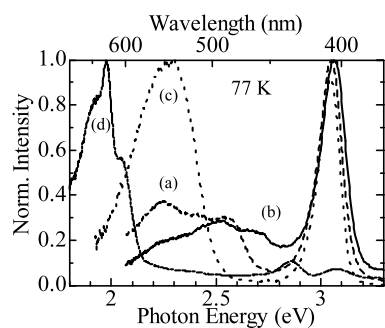


Fig. 16. Examples of EL spectra at visible wavelength region: PHPPS-coumarin 6 (2 mol.%), (b)PHPPS-erylene (1 mol.%), (c)PHPPS-DCM (2 mol.%) and (d) PHPPS-ZnTPP (2 mol.%).

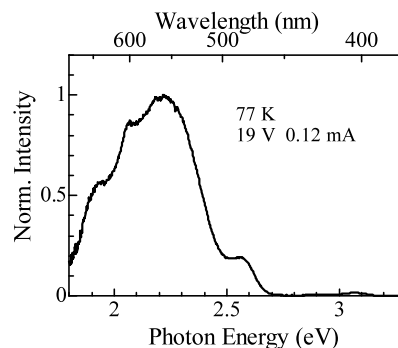


Fig. 17. An EL spectrum of the PHPPS-mixed dye-EL device with perylene (5.0 mol.%), coumarin 6 (2.5 mol.%), DCM (1.0 mol.%) and ZnTPP (0.2 mol.%) at 77 K.

emission including blue, green and red wavelength region.

The intensity of PHPPS emission decreased remarkably in Fig. 17. Together with our PL and PLE results, we consider that the main energy flow of this white EL comes from PHPPS through resonant energy transfer. Designing EL spectrum simply by intermixing dye molecules in solution is a promising way for improving productivity of EL devices, though energy transfer among dye molecules must be also included in a more detailed analysis.

We would like to point out that the conducting properties of polysilane as a molecular wire lead us to wide fields of applications, not only for light emitting devices but also for photo-detectors. Combining polymethylphenylsilane with suitable dye molecules, a photoconductive film with wavelength selectivity has been achieved recently [30].

6. Suppression of photo-oxidation

One of the most serious problems for practical applications of polysilanes is the photo-oxidation of Si main-chain under UV light irradiation. Since a long and emissive segment tends to suffer the photo-oxidation, originally efficient light emission of polysilane decreases rapidly during UV light exposure. Suppression of the photo-oxidation has been tried by embedding polysilane into SiO₂ glass network. Originally hydrophobic polysilanes were coupled to hydrophilic molecules in order to introduce them into sol-gel glass [31].

We synthesized water-soluble polysilanes by Wurtz-type reaction and Friedel-Crafts chloromethylation [23]. Shown in Fig. 18 are molecular structures of synthesized poly-*n*-hexyl(((*N,N*-dimethyl-3-methylpentan-1-ol-2-ammonio)methyl)phenyl) silane chloride (HSC), poly-*n*-propyl((triethylammonio)methylphenyl)silane chloride (PSC), and poly-*n*-hexyl(((triethylammonio)methyl)phenyl)propylsilane chloride (HTSC), respectively.

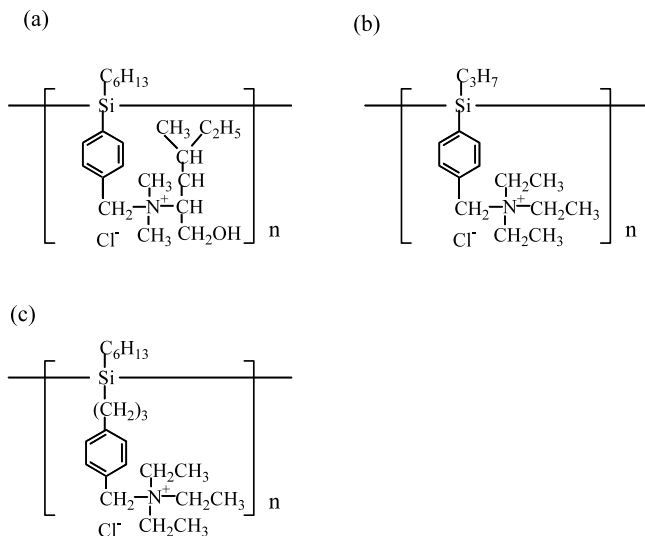


Fig. 18. Molecular structure of synthesized water-soluble polysilanes: (a) HSC, (b) PSC and (c) HTSC.

Through conventional sol-gel process [24,25], ethanol-diluted polysilane (HSC, PSC or HTSC) was added to the starting solution of tetraethoxysilane. The solution was spin-coated on quartz substrates, dried for 1 week at room temperature, and then heated up to 80 °C for 90 min to form a SiO₂ glass film containing HSC, PSC or HTSC. The composition of the polysilane was set at 2 mol.% when compared by Si numbers.

The PL and PLE spectra of HTSC embedded into sol-gel glass were identical to those of spin-coated HTSC film, showing that the main-chain is sufficiently relaxed even inside glass network. The PL intensity change during UV light irradiation is shown in Fig. 19. We introduced poly-dimethylsiloxane (PDMS) in addition

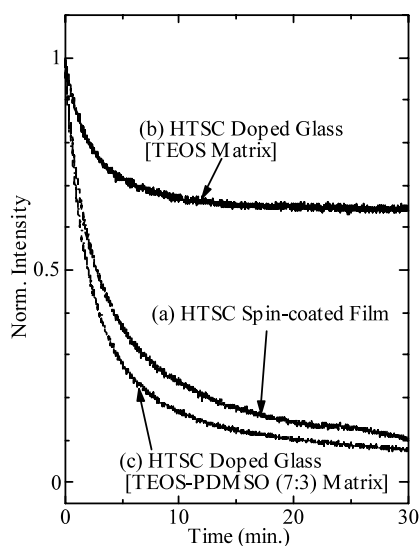


Fig. 19. PL intensity decrease of HTSC-doped glass (solid curve), HTSC and PDMS-doped glass (dashed curve) and HTSC spin-coated film (dotted curve) as a function of time. The excitation condition is 45 $\mu\text{W cm}^{-2}$ at 4.0 eV.

to HTSC in one glass film in order to distort the conformation of HTSC. The glass film with both PDMS and HTSC, and HTSC spin-coated film showed a PL quenching down to 10% of their initial values after 30 min. The PL intensity of the glass film with HTSC quenched down during initial 10 min, but the intensity was kept at 70% and no additional decrease was observed even after 30 min. This distinct difference is attributed to an effective protection of surrounding SiO₂ glass network against free oxygen and water, and an effect of restoration from a metastable state during photo-oxidation. The difference between the glass film including PDMS implies that water-solubility of the polysilane itself is essential for the microscopic adaptability toward SiO₂ glass network. Si-based organic and inorganic hybridization is also an important field for polysilanes on this respect.

7. Conclusion

We have studied radiative properties and the energy transfer process of polysilanes. Originating from one-dimensional configuration, polysilane has high efficiency of resonant energy transfer between energy-matched counterparts even without molecular alignment. In addition to conductive properties, such advantage was utilized for EL applications. We observed EL of perylene (blue), coumarin 6 (green), DCM and ZnTPP (red), and also their mixture (white) via the energy transfer from PHPPS.

Considering high oscillator strength and conductivity by σ -conjugated one-dimensional configuration, wide range of selecting side-chains, compatibility with SiO₂ glass and crystalline Si substrate, low cost and low environmental disturbance, etc., polysilanes have a possibility to open new fields of Si-based optical applications.

Acknowledgements

The authors would like to thank Dr Ken Hatano for intuitive discussion and experimental support, Mr Nobuhiko Gokan and Mr Tetsuo Koyama for providing quantitative analyses, Mr Youhei Tanaka for assisting research. They also thank Hosono Bunka-Kikin, Iketani Foundation and Japan Society for the Promotion of Science for their financial supports.

References

- [1] R. West, *J. Organomet. Chem.* 300 (1986) 327.
- [2] T. Kagawa, M. Fujino, K. Takeda, N. Matsumoto, *Solid State Commun.* 57 (1986) 635.

- [3] R.G. Kepler, J.M. Zeigler, L.A. Harrah, S.R. Kurtz, *Phys. Rev. B* 35 (1987) 2818.
- [4] M. Fujino, *Chem. Phys. Lett.* 136 (1987) 451.
- [5] R.D. Miller, J. Michl, *Chem. Rev.* 89 (1989) 1359.
- [6] K. Furukawa, M. Fujino, N. Matsumoto, *Macromolecules* 23 (1990) 3423.
- [7] H. Tachibana, M. Matsumoto, Y. Tokura, Y. Moritomo, A. Yamaguchi, S. Koshihara, R.D. Miller, S. Abe, *Phys. Rev. B* 47 (1993) 4363.
- [8] Y. Majima, Y. Kawata, Y. Nakano, S. Hayase, *J. Polym. Sci.* 35 (1997) 427.
- [9] Kamata, S. Aihara, W. Ishizaka, M. Umeda, D. Terunuma, K. Yamada, S. Furukawa, *J. Non-Cryst. Solids* 227–230 (1998) 538.
- [10] Nakayama, S. Nonoyama, *Solid State Comm.* 92 (1994) 591.
- [11] C.W. Tang, S.A. VanSlyke, *Appl. Phys. Lett.* 51 (1987) 913.
- [12] A. Fujii, K. Yoshimoto, M. Yoshida, Y. Ohmori, K. Yoshino, *Jpn J. Appl. Phys.* 34 (1995) L1365.
- [13] H. Suzuki, *Adv. Mater.* 8 (1996) 657.
- [14] K. Ebihara, S. Koshihara, T. Miyazawa, M. Kira, *Jpn J. Appl. Phys.* 35 (1996) L1278.
- [15] S. Aihara, W. Ishizaka, M. Umeda, A. Nishibori, N. Kamata, D. Terunuma, K. Yamada, *Conv. Jpn Soc. Appl. Phys.* (1997) 2a-ZQ-10 (in Japanese).
- [16] S. Aihara, N. Kamata, W. Ishizaka, M. Umeda, A. Nishibori, D. Terunuma, K. Yamada, *Jpn J. Appl. Phys.* 37 (1998) 4412.
- [17] S. Aihara, N. Kamata, A. Nishibori, H. Satoh, K. Nagumo, D. Terunuma, K. Yamada, *Proceedings of the International Symposium on Organosilicon Chemistry 2D32*, 1999, pp. 105.
- [18] S. Aihara, N. Kamata, A. Nishibori, K. Nagumo, H. Satoh, D. Terunuma, K. Yamada, *J. Lumin.* 87–89 (2000) 745.
- [19] R. Ishii, H. Satoh, S. Tonsyo, N. Kamata, D. Terunuma, S. Furukawa, *Proc. IEICE OME2001-8*, 2001, pp. 43 (in Japanese).
- [20] S. Aihara, N. Kamata, M. Umeda, K. Kanezaki, K. Nagumo, D. Terunuma, K. Yamada, *Opt. Rev.* 6 (1999) 393.
- [21] N. Kamata, R. Ishii, Y. Yaoita, S. Tonsyo, D. Terunuma, S. Furukawa, *Proc. 2001 Electronics Society Conf. of IEICE, SC-6-8*, 2001, pp. 159.
- [22] N. Kamata, R. Ishii, S. Tonsyo, D. Terunuma, *Appl. Phys. Lett.* 81 (2002) 4350.
- [23] D. Terunuma, K. Nagumo, N. Kamata, K. Matsuoka, H. Kuzuhara, *Polym. J.* 32 (2000) 113.
- [24] H. Satoh, S. Aihara, S. Okutsu, Y. Yaoita, N. Kamata, D. Terunuma, *Conv. Jpn Soc. Appl. Phys.* (2000) 29a-T-17 (in Japanese).
- [25] H. Satoh, N. Kamata, K. Kanezaki, S. Aihara, Y. Yaoita, D. Terunuma, *Proc. Int. Conf. on Physics of Semiconductors*, Springer Proc. in Physics, 87 (2001) 1669.
- [26] Th. Forster, *Ann. Physik* 2 (1948) 55.
- [27] D.L. Dexter, *J. Chem. Phys.* 21 (1953) 836.
- [28] F.W. Embs, G. Wegner, D. Neher, P. Albouy, R.D. Miller, C.G. Willson, W. Schrepp, *Macromolecules* 24 (1991) 5068.
- [29] L.S. Hung, *Appl. Phys. Lett.* 70 (1997) 152.
- [30] S. Aihara, Y. Hirano, T. Tajima, K. Tanioka, M. Abe, N. Saito, N. Kamata, D. Terunuma, *Appl. Phys. Lett.* 82 (2003) 511.
- [31] K. Matsukawa, S. Fukui, N. Higashi, M. Niwa, H. Inoue, *Chem. Lett.* (1997) 1073.